Non-Gaussian behavior in jamming / unjamming transition in dense granular materials

A. P. F. Atman[*], E. Kolb[†], G. Combe[**], H. A. Paiva[‡] and G.H.B. Martins [§]

[*]*Departamento de Física e Matemática and National Institute of Science and Technology for Complex Systems, Centro Federal de Educação Tecnológica de Minas Gerais, CEFET–MG, Av. Amazonas 7675, 30510-000, Belo Horizonte, MG, Brazil.*
[†]*PMMH, CNRS UMR 7636, UPMC and Université Paris Diderot, ESPCI-ParisTech, 10 rue Vauquelin, 75231 Paris Cedex 05, France*
[**]*Laboratoire 3S-R (Sols,Solides,Structures - Risques) UMR 5521 (UJF, INPG, CNRS) BP 53, Grenoble, France.*
[‡]*Departamento de Física e Matemática, CEFET–MG.*
[§]*Departamento de Engenharia Elétrica, CEFET–MG.*

Abstract. Experiments of penetration of a cylindrical intruder inside a bidimensional dense and disordered granular media were reported recently showing the jamming / unjamming transition. In the present work, we perform molecular dynamics simulations with the same geometry in order to assess both kinematic and static features of jamming / unjamming transition. We study the statistics of the particles velocities at the neighborhood of the intruder to evince that both experiments and simulations present the same qualitative behavior. We observe that the probability density functions (PDF) of velocities deviate from Gaussian depending on the packing fraction of the granular assembly. In order to quantify these deviations we consider a q-Gaussian (Tsallis) function to fit the PDF's. The q-value can be an indication of the presence of long range correlations along the system. We compare the fitted PDF's obtained with those obtained using the stretched exponential, and sketch some conclusions concerning the nature of the correlations along a granular confined flow.

Keywords: jamming/unjamming transition, granular systems, q-gaussian distributions, flow in channels
PACS: 81.05.Rm, 05.10-a, 83.50.Ha

INTRODUCTION

Due to its importance for technological applications as well for better understanding of natural phenomena, in last years increasing interest has been paid on the so-called jamming/unjamming transition in confined granular systems [1, 2, 3, 4, 5]. Of particular interest is the clogging of granular material around an intruder – or obstacle– which is a quite common situation in the industry (transport and confining materials) or civil engineering (pile driving for deep foundations). From the mechanical point of view, this type of experiment may provide a better understanding of yielding in granular media by observing directly the structural and dynamic features of the mechanisms which govern the plasticity in dense granular media [4, 5, 6]. Thus, the study of the rheology of a confined granular system close to the jamming became one of the key points of current research, and one of the fundamental issues on current research is to characterize the velocity distribution which governs the system at different jamming/unjamming situations. It is well known that, assuming molecular chaos hypothesis, the expected distribution for a set of colliding particles is that from Maxwell-Boltzmann theory, the Gaussian distribution with its typical bell-shape format and, indeed, it is observed in dilute granular systems and granular gases [7, 8]. However, previous studies in different confining situations (jamming) [9, 10, 11] have shown that the measured distribution usually deviates a lot from the Gaussian, and the function generally used to fit the data in this scenario is the stretched exponential [12, 13].

In this work, we propose to investigate the grain velocities' distribution around the intruder as a function of the packing fraction of the granular system, in order to verify a possible connection between the characteristic exponent of the distribution and the degree of jamming. We have fitted the data by two kinds of probability distribution functions (PDF's). First, we have considered the stretched exponential,

$$f_\alpha(x) = A * exp(B * (x - x_0)^\alpha) \ , \quad (1)$$

where A, B, and x_0 are free parameters usually employed in the fit function, and α is the degree of the distribution. Second, we have used the q-Gaussian which was proposed by C.Tsallis [14] as a generic distribution to describe pdf in non-extensive systems:

$$f_q(x) = \frac{\sqrt{(D)}}{C}(1 - Dx^2(1-q))^{\frac{1}{1-q}} \ , \quad (2)$$

where D is an adjustable parameter (analogous to the inverse of temperature in the Boltzmann-Gibbs formula-

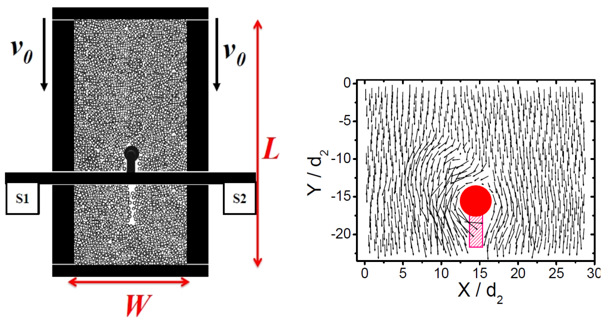

FIGURE 1. Schematic of the experiment. The containing box of dimensions $W = 54\ d_2$ and $L \leq 94\ d_2$ is placed horizontally over a translating plate and filled with the bidisperse mixture with $7:4$ proportion of large to small disks. The arrows on both sides indicate the movement of the box at velocity v_0; the small circle in the middle marks the intruder, which is fixed in the laboratory frame and connected to two force sensors S1 and S2. The right panel shows a typical displacement map obtained between two successive snapshots with a magnification factor of 50.

tion) and C is a normalization factor. In the fitting procedure, we let D and C vary as free parameters. For tangential velocity distributions for q-gaussian as well as for stretched exponential fits, we also included a 4^{th} parameter, x_0 in order to consider distributions not centered at the origin. The parameter q, which gives the name of this q-Gaussian PDF, is the control parameter which allows to recover the usual Gaussian distribution when $q = 1$, while for $q > 1$ we should expect long range correlations along the system. The major advantage of this particular choice for the PDF is its ability to fit all the data range with a single function, and no need to use a combination of stretched exponential and Gaussian to fit separately the tail and the central part of the distribution [3]. Another interesting feature of the q-Gaussian is the possibility to link directly the value of the q to the length of correlations along the system. For $q = 1$, we expect short range correlations, as assumed in the molecular chaos hypothesis; for $q > 1$, long-range correlations should arise in the system, and the distribution exhibits heavy tails. Thus, we expect that for unjammed, looser systems, the velocity distribution should be rather well described by Gaussian functions or q-Gaussians with $q \to 1$, while for jammed situations we expect to find a good fit with $q > 1$.

The paper is structured as the following: in the next section we present the experimental set up and the simulation method, and the analysis technique to build the distributions. Next, we compare the fitted exponent values for the experiments and simulations, and their dependence with the packing fraction ϕ and temporal evolution. Finally, we sketch some conclusions.

METHODOLOGY

The experimental setup was already presented in details previously [5] and consists in an horizontal rectangular box filled with a bidisperse mixture of grains – see Figure 1. with $d_2 = 1.25\ d_1$, where d_2 (d_1) is the diameter of the large (resp. small) species. In the experiments shown, typically around ~ 6500 grains were used. The packing fraction ϕ was adjusted to $0.8 < \phi < 0.84$, typically below or equal the jamming packing fraction for a frictional granular medium. A CCD camera of 1600×1200 pixels placed above the set-up recorded images every $d_2/30$ displacement of the box, while the box was pulled at a constant velocity v_0 along the tangential t direction. Then an image analysis software is used to localize the positions of grains in each image. By calculating the displacement of each grain between successive images, we construct the cumulative velocity PDF and fit with the q-Gaussian function and stretched exponential, as shown in Figure 2. More precisely, we measured the velocity distributions along the normal v_n and tangential v_t directions of box displacement. We used a minimum square method to obtain the best fit values for the PDF's using equations 1 and 2 as fitting functions.

The simulation is designed to be closer as possible to the experimental situation. We have used a molecular dynamics (MD) code in 2 dimensions, with velocity Verlet implementation and 3^{rd} order Gear predictor-corrector [15]. The rheology for the particles was a modified version of the original Cundall-Strack model [16], with the contact between grains represented as normal and tangential springs, and Coulomb friction between grains. The simulated system has the same geometry, number of grains and aspect ratio as the experimental setup, but the range of packing fraction values simulated was a bit different from the experiments, since we can better explore the parameter space with simulations. Besides, the microscopic parameters were chosen in order to get the best performance for the code, and do not correspond literally to the values expected if a direct conversion of the experimental values was made. Thus, in normalized unities the values used for the parameters were: $k_n = 1000$, $k_t = 750$ for the normal and tangential spring stiffnesses, and $\mu = 0.5$ for the friction coefficient. We have used a critical damping in the normal direction of the contacts, but no damping in the tangential one, only Coulomb friction dissipates energy in tangential contact direction. (Please find in [17] the precise definitions of the normalized unities and in [18] more details concerning the simulation method. The normalization of length used here was the width of the system, W).

We ran simulations with the same number of realizations as performed in the experiments. Then we averaged the same number of snapshots to build the velocity pdf's (the "snapshots" in simulations correspond to the config-

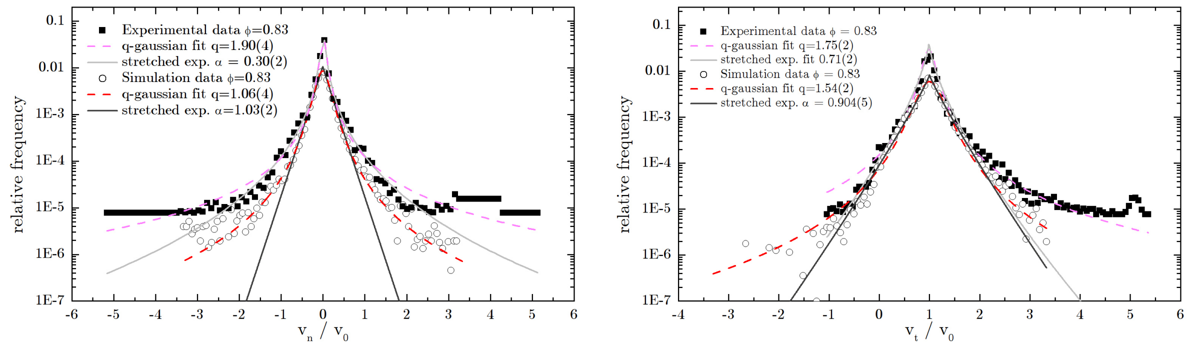

FIGURE 2. Velocities PDF's for experimental data and simulations. The distribution along the normal direction of displacement is shown at left while the distribution along the tangential direction is shown at right.

urations taken at the same frequency as in the experiment – at each $d_2/30$ displacement of the box. Thus, we were able to compare directly simulations with experimental data - Figure 2.

The distributions usually considered about 160 consecutive snapshots, and we averaged the velocities obtained from the displacements calculated between 2 consecutive snapshots (please find interesting features when different values of snapshots are used to calculate the displacement [19]). A typical experiment runs along 1600 snapshots and we can obtain the temporal evolution of the distribution. We show here only the results for distributions taken in front of the intruder in a region corresponding to the right panel of Figure 1. We study the temporal evolutions of the best fit parameters for the two PDF's used to fit the data as well the dependence of the fitted value at the half time of the experiment in function of the initial packing fraction ϕ.

DISCUSSION

In figures 2 we show some results for the velocities PDF's at the same packing fraction, for experiments and simulations. Despite not observing a perfect match, most of the qualitative features observed in the experimental PDF's were successfully reproduced by simulation and, sometimes, even quantitatively. For example, the distributions for $v_{n,t}/v_0 < 1$ show a remarkable match. Moreover, some observations were common to all packing fractions:

- First, it is clear that the confinement provoked by the presence of the intruder induces strong correlations for grains velocities, expressed by heavy tail distributions.
- Due probably to the box aspect ratio, longer than wider, we observe that the confining effect – jamming – is stronger in the normal velocities distribution than in tangential one. Thus, we have systematically verified that the stretched exponential fits v_n distributions better than q-Gaussian, since the systems are almost completely correlated along this direction.
- The v_t distributions were frequently asymmetrical, with heavy tails with different sizes for $v_t/v_0 > 1$ and $v_t/v_0 < 1$. The long heavy tails for $v_t/v_0 > 1$ systematically were better fitted by q-Gaussian.

The asymmetry observed in the tangential case can be explained considering the rectangular region of snapshot around the intruder: since the intruder is placed in the central bottom part of the region, most of the particles in average were placed in front of the intruder and moving with the same velocity as the box. As they approached the intruder, due to the flux conservation in average, the grains gained velocity, and competed to pass aside the intruder. Other grains which are located just in front of the intruder slowed down, and an excess of small velocities is observed in the distributions. The recirculation of grains just in the vicinity of the intruder (see the right panel in Figure 1) contributes for the negative values of velocities.

Another feature is the excess of velocities for experimental distributions close to $v_t/v_0 = 1$ and $v_n/v_0 = 0$, compared with simulations. This is probably due to the limited experimental frame of observation: When a new grain enters in the window observation, its preceding position is not known. Thus its first velocity is arbitrarily set to 0 in normal direction and to v_0 in the tangential one. Therefore we systematically observe an excess of velocities v_n close to zero or v_t close to v_0 in experiments compared with simulations where all the velocities are known, even outside the window observation.

Figure 3 shows the temporal evolution of the fitted parameter q from the q-Gaussian PDF's at the same value of packing fraction. We observe that the values obtained in the experiments are almost constant (except at the

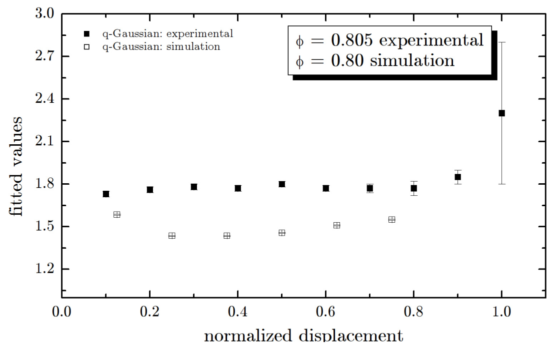

FIGURE 3. Temporal evolution of the exponents of the PDF's used to fit the data, for the packing fraction $\phi = 0.805$ in the experimental case, and $\phi = 0.8$ in simulation. Both plots show the q-Gaussian best fit for v_t in function of the normalized displacement of the containing box.

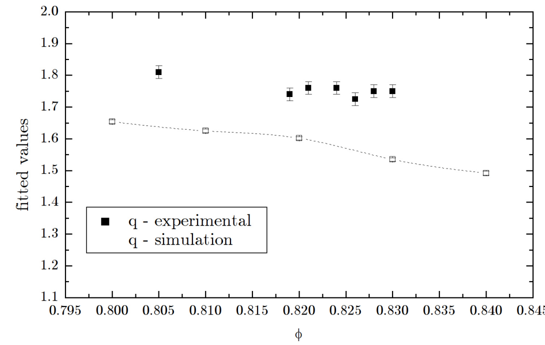

FIGURE 4. Dependence of the fitted values with the packing fraction. The best fitted values of the pdf used - q-Gaussian - were shown in function of the packing fraction at the half-time of the experiment, for v_t distribution.

end of travelling), while in the simulations we observe a rather small but non-monotonic variation with time.

Figure 4 shows results for the fitted exponents q in function of the packing fraction. Clearly, the simulation data show a clear tendency for $q \to 3/2$ as the packing fraction increases. The experimental results, however, do not show clearly this feature, which could be due to he excess of experimental velocity v_t close to v_0, as previously discussed. Another possible explanation, is the absence of friction between grains and the table in the case of the simulation. In simulations, since we considered the 2D case, we have no manner to implement this friction.In the experiments, the region in front of the intruder attains progressively a critical packing fraction as the box moves, and we can observe voids and inhomogeneities in the packing of grains. In simulations, the system is considerably more homogeneous, and maybe it can explain why the simulation displays monotonic dependence on the values of the fitted parameters with the packing fraction while the experimental results are inconclusive.

CONCLUSIONS AND PERSPECTIVES

We have presented experimental and simulation results for the velocity PDF's of confined granular systems in the presence of an intruder. We fit the data with q-Gaussian and stretched exponential functions, and sketch the temporal evolution of the fitted values. We verified that the system exhibits strong correlations in both normal and tangential directions, expressed by the $q > 1$ and $\alpha < 1$, but we could not verify quantitative concordance between the simulations and experiments. In simulations, a clear monotonic tendency was verified, pointing to $q \to 3/2$ and $\alpha \to 1$ as ϕ increases, but the experimental values do not display any clear tendency.

ACKNOWLEDGMENTS

APFA and GHBM thanks FAPEMIG and CNPq for financial support. APFA and GC thanks CEFET and Université Joseph Fourier for making possible a 3 month invited professor grant.

REFERENCES

1. R. P. B. H. M. Jaeger, S. R. Nagel, *REV MOD PHYS* **68**, 1259 (1996).
2. M. S. Y. Murayama, *J PHYS SOC JAP* **67**, 1826 (1998).
3. P. R. N. S. Moka, *PHYS REV LETT* **95**, 068003 (2005).
4. J. L. P. C. E. C. E. Kolb, J. Cviklinski, *PHYS REV E* **69**, 031306 (2004).
5. N. G. P. Cixous, E. Kolb, and J.-C. Charmet, *Powders and Grains 2009* **AIP Conference Proceedings 1145**, 539 (2009).
6. A. L. E. K. J. C. J. L. E. C. G. Caballero, E. Kolb, *J PHYS COND MATT* **17**, S2503 (2005).
7. F. C. M. J.S. van Zon, *PHYS REV LETT* **93**, 038001 (2004).
8. J. S. O. J. S. Urbach, *PHYS REV E* **60**, R2468 (1999).
9. A. K. D. L. Blair, *PHYS REV E* **64**, 050301(R) (2001).
10. A. K. A. V. Orpe, *PHYS REV LETT* **98**, 238001 (2007).
11. H. H. A. Kawarada, *J PHYS SOC JAP* **73**, 2037 (2004).
12. N. M. F. Rouyer, *PHYS REV LETT* **85**, 3676 (2000).
13. A. V. A. Puglisi, F. Cecconi, *J PHYS COND MATT* **17**, S2715 (2005).
14. C. Tsallis, *BRAZ J PHYS* **39**, 337 (2009).
15. D. T. M.P. Allen, *Computer simulation of liquids*, Oxford University Press, Oxford, 1987.
16. O. S. P.A. Cundall, *GEOTECHNIQUE* **29**, 47 (1979).
17. G. C. A.P.F. Atman, P. Claudin, *COMP PHYS COMM* **180**, 612 (2009).
18. J. G. G. R. G. C. P. C. R. P. B. E. C. A. P. F. Atman, P. Brunet, *J PHYS COND MATT* **17**, S2391 (2005).
19. G. V. V. Richefeu, G. Combe, *GÉOTECH LETT* **2**, 113 (2012).